

Tuning the face orientation of ZnO nano/microcrystals by a wet chemical method

Aparna Thankappan^{1,2*}, Sheenu Thomas¹, and V. P. N. Nampoory¹

¹International School of Photonics (ISP), Cochin University of Science and Technology, Kochi, India

²Inter University Centre for Nanomaterials and Devices (IUCND), Cochin University of Science and Technology, Kochi, India

*Corresponding author: aparna.subhash@gmail.com

Received April 5, 2013; accepted August 2, 2013; posted online September 25, 2013

We successfully synthesize four kinds of ZnO nano/microcrystals including dumbbell microrods, nanoflakes, nanoplates, and microrods by a simple wet chemical method. Growth duration is found to play a crucial role in the morphologies of these ZnO nano/microcrystallites. In addition, growth conditions are systematically studied as a function of precursor concentration and temperature. The structural and optical characteristics of the ZnO samples are further investigated by X-ray diffraction, scanning electron microscopy, and photoluminescence spectroscopy.

OCIS codes: 180.5810, 300.6470.

doi: 10.3788/COL 201311.101801.

Control over the morphology and structure of nanomaterials is essential for the development of future devices^[1]. Over the past few years, considerable effort has been exerted in controlling the morphology of nanocrystals to fine tune their properties for potential applications because the size, orientation, morphology, aspect ratio (width-to-length ratio), and even crystal density can significantly influence various properties. Therefore, the morphology-controlled synthesis of nanostructures must be developed^[2] to address the demand for exploring the potentials of ZnO.

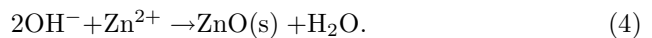
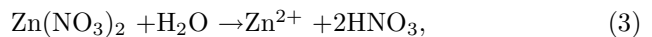
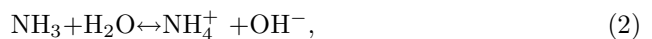
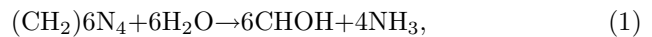
Among promising optoelectronic semiconductors, ZnO is a key functional material exhibiting ultraviolet (UV) photoluminescence emission, transparent conductivity along with semiconductivity, magnetic properties, and piezoelectric properties. ZnO also has a wide band gap with an energy of 3.37 eV, notable biocompatibility, as well as excellent chemical, mechanical, and thermal stabilities^[3]. Thus, ZnO is attracting attention from fundamental and practical researchers. ZnO is a polar crystal with hexagonal phase and high anisotropy that leads to oriented growth along the c-axis^[4]. Crystal growth morphology results from the interplay between crystallographic anisotropy and growth kinetics^[5]. Anisotropy is a basic property of crystals. Anisotropic tendency during crystal growth in association with the relationship between crystal planes of solid materials and their physicochemical properties has been studied by several researchers^[6]. Given the poor morphology-controlled syntheses of nanoscale metal oxides, systematic studies on the connection between crystal planes and properties are limited. Morphology-controlled syntheses can clearly demonstrate the strong excitation wavelength dependence of the fluorescence emission of ZnO crystals. The excitation wavelength-dependent features of fluorescence emission allows for tunable laser sources.

In this letter, we report on the controlled synthesis of the ZnO nano/microcrystals with different morphologies using a simple wet chemical method. Dumbbell (DB)

microrods, nanoflakes, nanoplates, and microrods with good crystalline properties were synthesized at different growth durations (6–22 h) with excellent reproducibility. The influences of precursor concentration, reaction time, and temperature on the size and morphology of ZnO were investigated. Scanning electron microscopy (SEM) reveals that the morphology of ZnO can be effectively controlled as DB microrods, nanoflakes, nanoplates, and microrods. X-ray diffraction (XRD) measurements show that all samples have a hexagonal phase structure. The room temperature photoluminescence of the as-prepared ZnO is found to significantly depend on crystal size, orientation, morphology, aspect ratio, and crystal density.

All chemicals were purchased from Merck Ltd. And used as received without further purification. A nutrient solution was prepared from an aqueous solution of zinc nitrate hexahydrate ($\text{Zn}(\text{NO}_3)_2 \cdot 6\text{H}_2\text{O}$) and hexamethylenetetramine (HMTA) ($(\text{CH}_2)_6\text{N}_4$). A hexamine solution was added dropwise to the zinc nitrate solution while stirring.

The following reactions are involved in the crystal growth of ZnO^[7]



The reaction decomposes HMTA to formaldehyde (HCHO) and ammonia (NH_3), which acts as a pH buffer by slowly decomposing to provide a gradual and controlled supply of NH_3 . Then, NH_3 forms ammonium hydroxide and support OH^- ^[8]. Finally, OH^- anions react with Zn^{2+} cations to form ZnO. Precursor concentration, time, and temperature dependence experiments were carried out to investigate the growth processes of ZnO.

The size and morphology of ZnO samples were characterized by SEM (JSM6390, JEOL/EO, USA). XRD data

were collected on an AXS Bruker D ϕ diffractometer using Cu K α radiation ($\lambda = 0.1541$ nm). The operating conditions were 35 mA and 40 kV at a step of 0.020° and a step time of 29.5 s within the 2θ range of 30° – 70° . Fluorescence emission was measured using a Cary Eclipse fluorescence spectrometer (Varian).

The growth mechanism of ZnO crystals are then elucidated by a detailed analysis of the experimental results. The growth mechanism enables control over ZnO crystals and is essential for tailoring the optical, electrical, and magnetic properties of crystals for certain applications.

The morphology of the ZnO crystals synthesized at a controlled growth rate for 6, 11, 18, and 22 h is revealed by SEM shown in Fig. 1. All obtained ZnO samples have a wurtzite structure (hexagonal phase, space group P6 $_3$ mc). The XRD patterns of ZnO with typical morphologies are shown in Fig. 2. All diffraction peaks are well assigned to hexagonal-phase ZnO reported in a JCPDS card. The summarized morphologies and reaction conditions are illustrated in Table 1. When the reaction medium was heated at 80 °C for 6 h, ZnO DB microrods with an average diameter of 800 nm and length of 3 μ m are formed. The ZnO DB microrods preferentially grow along the [0001] direction and form similar to the sharing of two individual microrods, stabilizing between Zn [0001] planes and with Zn [0001] faces masked. The DB microrods also have a wider size distribution than nanoplates and nanoflakes. Peng *et al.*^[9] reported the precursor concentration-dependent structure morphology of ZnO nano/microcrystals. To understand the observed behaviors of ZnO, the growth mechanism must be studied. ZnO has a wurtzite crystal structure that is a polar molecule with [0001] polar surfaces and nonpolar [01 $\bar{1}$ 0] faces. The nonpolar surfaces are electrically neutral with a low surface energy, and the polar surfaces have a high surface energy, which is the main factor affecting the variation in growth rate along both polar and nonpolar directions^[10]. The length and width of the synthesized ZnO crystals are directly affected by the growth rate in the [0001] polar face and the [0110] nonpolar faces, respectively. With prolonged heating time for 11 h, the crystal growth along [0001] direction decreases, thereby leading to nanoflake formation. The DB ZnO microrods change into flake-shaped crystals because of the sequential dissolution of polar O [01 $\bar{1}$ 0] and non-polar [01 $\bar{1}$ 0] ones^[11]. When heated for

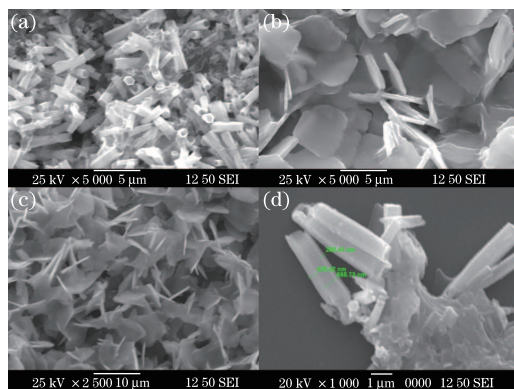


Fig. 1. Growth duration dependence of ZnO nanocrystals in Zn(NO $_3$) $_2$ 6H $_2$ O (1 mmol/L) and HMTA (1 mmol/L) solutions at 80 °C: (a) 6, (b) 11, (c) 18, and (d) 22 h.

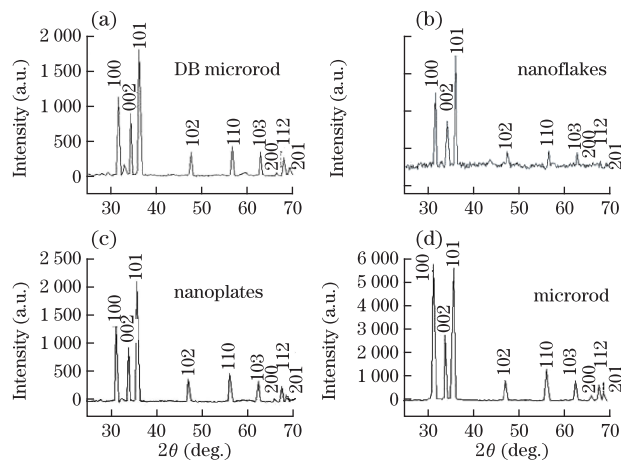


Fig. 2. XRD pattern of ZnO nano/microstructures: (a) DB microrods, (b) nanoflakes, (c) nanoplates, and (d) microrods.

Table 1. Crystalline Dimensions of DB Nanorods, Nanoflakes, Nanoplates, and Microrods

	Average Diameter (μ m)	Average Thickness (μ m)
DB Microrods	0.8	3
Nanoflakes	4	0.35
Nanoplates	4	0.2
Microrods	0.8	5

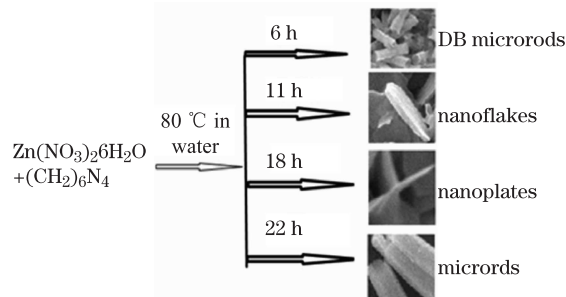


Fig. 3. Schematic of face orientation of ZnO nanostructures.

18 h, ZnO nanoplates with uniform size are fabricated in large scale; when heated for 22 h, microrods are observed. Surface reconstruction may favor a particular crystalline structure or surface orientation of a crystalline structure. The ZnO microrods are assumed to be formed by stacking of the nanoplates. Apparently, both DB microrods and hexagonal microrods have the same average diameter. A schematic of ZnO structures is shown in Fig. 3. We believe that growth duration plays a key role in the anisotropic growth of well-defined ZnO morphologies.

We also observed the variations in the molar concentration of the HMTA precursor solutions at zinc nitrate ratios of 1:0.5, 1:1, and 1:1.5. The aim was to determine the role of HMTA on DB microrod growth because this role is under debate. HMTA is a non-ionic cyclic tertiary amine that can act as a Lewis base to metal ions and as a bidentate ligand capable of bridging two zinc (II) ions in solution. HMTA is also known to hydrolyze, producing formaldehyde and ammonia within the pH and temperature range of ZnO rod reactions^[12]. The role of

HMTA in the synthesis procedure is to control the release of hydroxide ion during reaction, thereby tailoring the aspect ratio. Therefore, the concentration of OH^- anions is dominant factor affecting the growth process of ZnO nanorods. Adding hexamine at various concentrations to the zinc nitrate solution changes the pH from 5.89 to 6.04, as measured with a digital pH meter (MK VI). Thus, HMTA plays a key role in the growth of ZnO rods. The hydrolysis rate of $\text{C}_6\text{H}_{12}\text{N}_4$ is low and can provide OH^- anions at a steady rate, resulting in a solution with a constant concentration of OH^- anions. At low $\text{C}_6\text{H}_{12}\text{N}_4$ concentrations, the reaction rate of OH^- anions is low; at high $\text{C}_6\text{H}_{12}\text{N}_4$ concentrations, the reaction rate and growth rate of ZnO nanorods are high. The average diameter of the nanorod decreases with increased HMTA concentration in the solution, as shown in Fig. 4.

To study the effect of temperature on the ZnO DB microrods, DB microrods were grown at 70, 80, and 90 °C. The corresponding scanning electron micrographs of the rods grown at each temperature are shown in Fig. 5. Temperature is important in the growth control of ZnO nanostructures. The growth temperature affects the aspect ratio of the rods. The average length of the rods

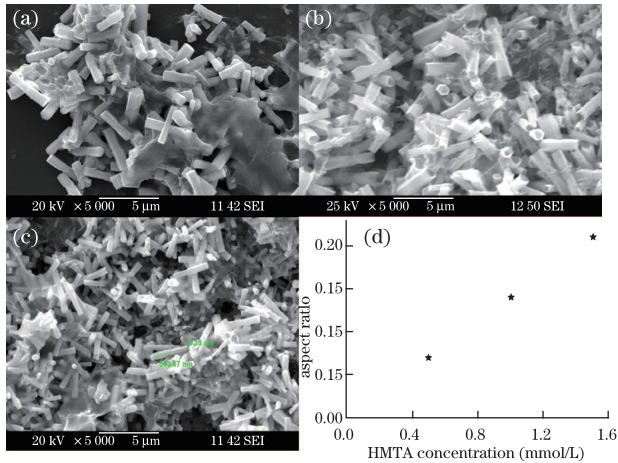


Fig. 4. HMTA concentration dependence of ZnO nanocrystals at 80 °C, 6 h in $\text{Zn}(\text{NO}_3)_2 \cdot 6\text{H}_2\text{O}$ (1 mmol/L) solutions: (a) 0.5, (b) 1, and (c) 1.5 mmol/L. (d) HMTA concentration versus aspect ratio.

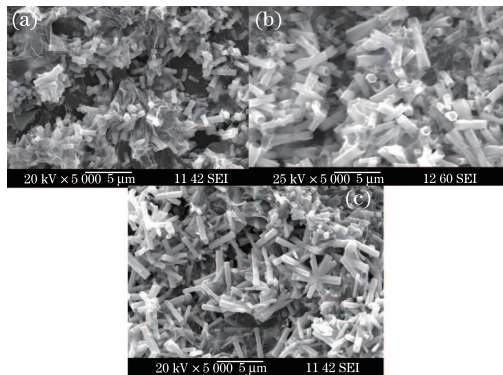


Fig. 5. Temperature dependence of ZnO nanocrystals in $\text{Zn}(\text{NO}_3)_2 \cdot 6\text{H}_2\text{O}$ (1 mmol/L) and HMTA (1 mmol/L) solutions for 6 h: (a) 70, (b) 80, and (c) 90 °C.

increases from 1.57 to 2.88 μm , and the average diameter decreases from 589 to 455.4 nm (measured with Digimizer, an affordable image analysis software) with increased temperature from 70 to 90 °C. The optimum temperature for obtaining high-quantity nanorods was found to be 80 °C. With increased temperature to 90 °C, HMTA more quickly decomposes than at a low temperature, thereby producing enough OH^- ions and resulting in sufficient size-controlled growth of ZnO with good aspect ratio compared with the other two. However, the alignment degree is poorer than that at 80 °C. This finding indicates that the growth rate is sensitive to temperature.

ZnO is a direct wide-band-gap (3.37 eV) semiconductor at room temperature with a large exciton binding energy (60 meV) suitable for effective UV emission. However, given the poor crystalline quality of nanomaterials such as high density of structural defects, impurities, etc., the UV emission band resulting from the recombination of excitons tends to be quenched and defect emission in the visible region is detected^[13]. These deficiencies hinder the broad use of ZnO in optoelectronic and lasing applications. Thus, photoluminescence spectra must be studied to evaluate the defects and optical properties of ZnO.

The photoluminescence of the obtained ZnO structures has different features depending on their morphological variations. The fluorescence behavior of ZnO nanostructures is studied as a function of the wavelength. The DB microrods, nanoplates, and nanoflakes exhibit UV peaks attributed to near-band-edge emission, and no defect emission is detected. The photoluminescence spectra of microrods recorded at various excitation wavelengths show striking differences in spectral features. The detailed emission spectra of ZnO structures are shown in the Fig. 6. The microrods give out blue-green fluorescence emission for the excitation wavelengths of 266 and 276 nm and excellent UV emission at 389.42 nm for the excitation wavelength of 286 nm. The green emission of ZnO microstructures centered at 530 nm is attributed to Zn^{2+} or O^{2-} vacancies and to the presence of extrinsic impurities or surface carriers. Our sample is grown at a low temperature of around 80 °C; thus, Zn^{2+} vacancies can be ruled out. Therefore, we assume that the emission at 530 nm is due to surface states excited along with $\text{h}_2\text{-e}_2$ and $\text{h}_3\text{-e}_3$ exciton formation and decay^[14,15]. This phenomenon also gives a series of lines at 387, 425, and 490 nm in addition to the green emission. Meanwhile, $\text{h}_1\text{-e}_1$ (low-energy exciton) selectively decays through emission at 387 nm because of the lower probability of interband transition of electron states^[16]. Clearly, crystal quality affects emission performance and thus the synthesized crystals with fewer defects exhibit enhanced UV emission intensity and reduced visible emission intensity.

In conclusion, we successfully synthesize DB microrods, nanoflakes, nanoplates, and microrods of ZnO with different ratios of polar-to-nonpolar faces through a simple, low-temperature wet chemical method. To finely modulate the morphology of ZnO, the relationship between morphologies and reaction conditions are investigated. Growth duration is found to play a crucial role in the face orientation of ZnO crystals. Moreover, precursor concentration and temperature have no

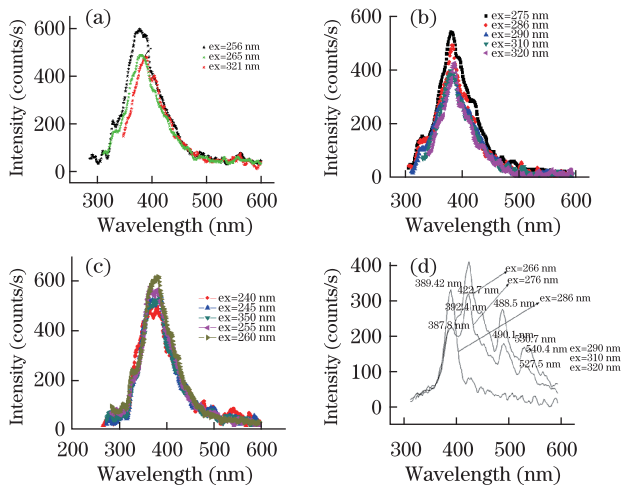


Fig. 6. Emission spectra of ZnO nano/microstructures: (a) DB microrods, (b) nanoflakes, (c) nanoplates, and (d) micro-rods.

obvious influence on the morphology and only slightly affects the size. The room-temperature photoluminescence of ZnO structures exhibit UV and visible emission depending on the morphology.

Author AT acknowledges the financial support of IUCND.

References

1. M. Lucas, Z. Wang, and E. Riedo, *Phys. Rev. B* **81**, 045415 (2010).
2. H. Yan, R. He, J. Pham, and P. Yang, *Adv. Mater.* **15**,

402 (2003).

3. O. Lupan, L. Chow, G. Chai, B. Roldan, A. Naitabdi, A. Schulte, and H. Heinrich, *Mater. Sci. Eng. B* **145**, 57 (2007).
4. H. Zhang, D. Yang, D. Li, X. Ma, S. Li, and D. Que, *Cryst. Growth Des.* **5**, 547 (2005).
5. G. Muller, J.-J. Metois, and P. Rudolph, *Crystal Growth from Fundamentals to Technology* (Elsevier, Amsterdam, 2004).
6. S. C. Navale, S. W. Gosavi, and I. S. Mulla, *Talanta* **75**, 1315 (2008).
7. T. Mahalingam, K. M. Lee, K. H. Park, S. Lee, Y. Ahn, J.-Y. Park, and K. H. Koh, *Nanotechnology* **18**, 035606 (2007).
8. J.-H. Tian, J. Hu, S.-S. Li, F. Zhang, J. Shi, X. Li, Z.-Q. Tian, and Y. Chen, *Nanotechnology* **22**, 245601 (2011).
9. W. Peng, S. Qu, G. Cong, and Z. Wang, *Cryst. Growth Des.* **6**, 1518 (2006).
10. B. Panigrahy, M. Aslam, D. S. Misra, and D. Bahadur, *Cryst. Eng. Comm.* **11**, 1920 (2009).
11. E. S. Jang, J.-H. Won, S.-J. Hwang, and J.-H. Choy, *Adv. Mater.* **18**, 3309 (2006).
12. L. E. Greene, B. D. Yuhas, M. Law, D. Zitoun, and P. Yang, *Inorg. Chem.* **45**, 7535 (2006).
13. M. Guo, P. Diao, and S. Cai, *J. Solid State Chem.* **178**, 1864 (2005).
14. C. Li, G. Fang, W. Guan, and X. Zhao, *Mater. Lett.* **61**, 3310 (2007).
15. J. Liu, X. Huang, K. M. Sulieman, F. Sun, and X. He, *J. Phys. Chem. B* **110**, 10612 (2006).
16. L. Irimpan, B. Krishnan, A. Deepti, V. P. N. Nampoore, and P. Radhakrishnan, *J. Phys. D Appl. Phys.* **40**, 5670 (2007).